Colloquia: WISH2010

Charged-particle multiplicity with ALICE at the LHC

D. Elia for the ALICE Collaboration

INFN, Sezione di Bari - Bari, Italy

Summary. — The pseudorapidity density and multiplicity distributions of charged
particles have been the first measurements carried out with the ALICE detector at
the LHC. After an introduction on the experiment and some details on the subde-
tectors relevant for these measurements, results from minimum bias proton-proton
collisions at 0.9, 2.36 and 7 TeV are presented. Comparisons with other measure-
ments and model predictions are also discussed.

PACS 12.38.Aw – General properties of QCD (dynamics, confinement, etc.).
PACS 25.75.Dw – Particle and resonance production.

1. – ALICE experiment at the LHC

ALICE is a general-purpose detector designed to measure the properties of strongly
interacting matter created in heavy-ion collisions at the CERN LHC. Several features,
such as low momentum cut-off and powerful tracking over a broad momentum range,
make it also an important contributor to the proton-proton LHC physics: here ALICE
aims both at setting the baseline for the understanding of the heavy-ion data and ex-
ploring the new energy domain [1].

The ALICE experimental apparatus has been designed as a dedicated heavy-ion de-
tector optimized to measure a large variety of observables in very high multiplicity en-
vironments with its performance able to resolve up to 8000 charged particles per unit of
rapidity. ALICE is able to detect and identify hadrons, leptons and photons over a wide
range of momenta. The whole detector, shown in fig. 1, consists of a central part (with
acceptance $|\eta| < 0.9$) to detect hadrons, electrons and photons, a forward spectrometer to
measure muons and additional smaller forward detectors for event characterization and
triggering. In the following the Silicon Pixel Detector (SPD) is briefly described since
it has been playing a key role for the first data and the charged-particle multiplicity
analysis: further details on the whole apparatus can be found in [2,3].

The SPD is the innermost part of the ALICE vertex and tracking system. It consists
of two cylindrical layers placed at 3.9 and 7.6 cm average radii, equipped with hybrid
silicon pixels for a total of about 9.8 M individual cells of size $50 \times 425\,\mu m^2$. It covers the
pseudorapidity ranges $|\eta| < 2$ and $|\eta| < 1.4$ with the inner and outer layer, respectively,
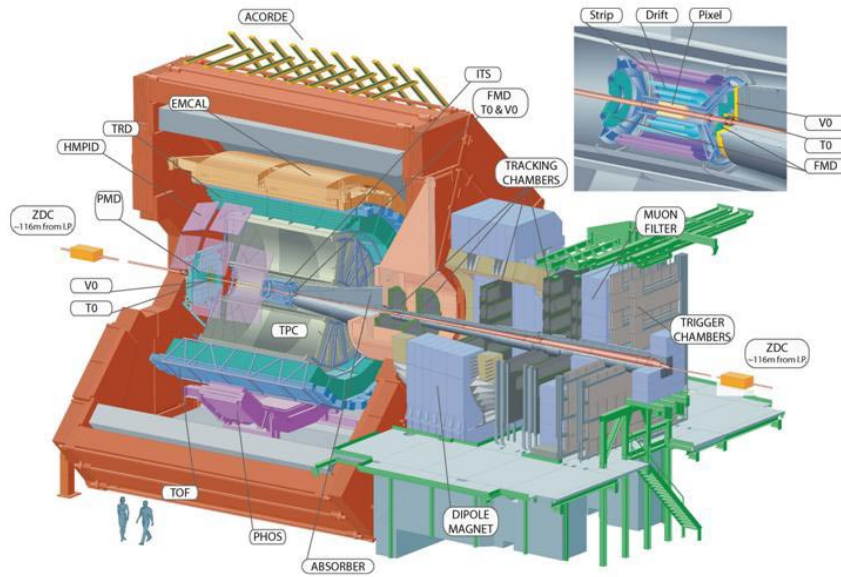
Fig. 1. – General view of the ALICE detector and details of the innermost silicon layers.

for particles originating in the centre of the detector. A fast signal (FastOR) is provided by each of the 1200 detector chips when at least one of its pixels is hit: all the FastOR signals are combined in a programmable logic unit which provides a level-0 trigger signal to the central trigger processor. The total number of active channels during the data taking was about 85%. The detector alignment has been obtained using both cosmic-ray tracks and tracks from proton-proton collisions [4].

2. – Tracklet reconstruction with the silicon pixels

Besides its key role as a vertex detector, the SPD allows to determine the number of charged primary particles in the central rapidity region. The basic steps of the reconstruction algorithm are described in the following.

First the position of the primary vertex is determined by correlating hits in the two SPD layers, then using the reconstructed vertex position as the origin, tracklets candidates are reconstructed: pairs of hits with one hit in each SPD layer are combined and the corresponding differences in azimuthal ($\Delta\varphi$, bending plane) and polar ($\Delta\theta$, non-bending direction) angles are computed. Good tracklets are then selected as hit combinations satisfying a cut on the sum of the squares of $\Delta\varphi$ and $\Delta\theta$ with a cut-off of 80 mrad and 25 mrad, respectively. In case different candidates share a hit in one of the two layers, only the combination with the smallest angular difference is taken as a good tracklet. The cut imposed on $\Delta\varphi$ would reject charged particles with transverse momentum below 30 MeV/c; however, the effective transverse-momentum cut-off due to absorption in the material is approximately 50 MeV/c.

The number of primary charged particles is obtained from the number of tracklets corrected for the following effects: trigger and vertexing efficiency, geometrical acceptance, detector and reconstruction efficiencies, undetected particles below the
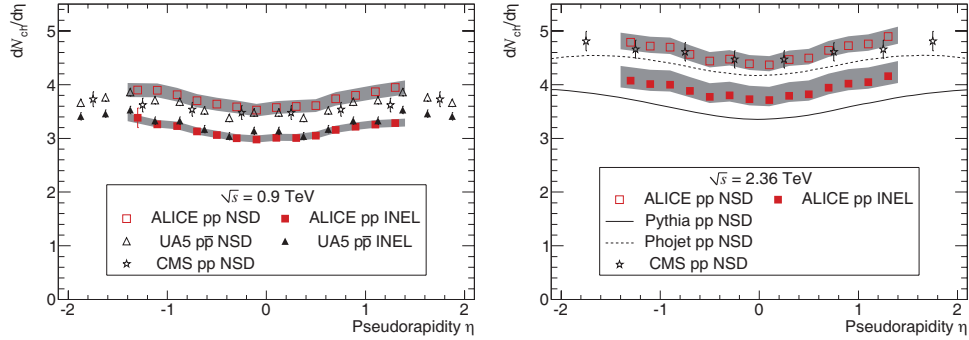
Fig. 2. – Left panel: pseudorapidity density distributions for INEL and NSD interactions at $\sqrt{s} = 0.9$ TeV, compared to UA5 and CMS data. Right panel: same for $\sqrt{s} = 2.36$ TeV data, compared to CMS results and predictions from PYTHIA and PHOJET [6].

transverse-momentum cut-off, background from secondaries. These effects and the corresponding corrections have been determined, using dedicated Monte Carlo productions, as a function of the z-position of the primary vertex and the pseudorapidity of the tracklet. Further details on the reconstruction and correction methods are given in [5,6].

3. – Pseudorapidity density and multiplicity distributions

ALICE has measured the charged-particle pseudorapidity density distribution with the very first low statistics sample of proton-proton collisions at a centre-of-mass energy $\sqrt{s} = 0.9$ TeV, provided by the LHC at the end of 2009 [5]. Results presented in this contribution are based on a larger statistics data sample at $\sqrt{s} = 0.9$ TeV as well as the first higher-energy collisions at 2.36 and 7 TeV, all from the 2010 run. Data at 0.9 and 7 TeV have been collected with a trigger requiring a hit in either one of the trigger scintillator counters (VZERO) or in the SPD detector (*i.e.* at least one charged particle anywhere in 8 units of pseudorapidity) in coincidence with signals from the two beam-pickup counters (BPTX). At 2.36 TeV the VZERO detector was turned off and the trigger required at least one hit in the SPD in coincidence with the BPTX.

Results at $\sqrt{s} = 0.9$ and 2.36 TeV are based on 150000 and 40000 collision events, respectively and are given for two different normalizations: inelastic (INEL), corresponding to the sum of all inelastic interactions, and non-single-diffractive (NSD), where the corrections for the two samples have been based on previous experimental data and Monte Carlo simulations. In the left panel of fig. 2 the charged-particle pseudorapidity density distribution for both INEL and NSD interactions at $\sqrt{s} = 0.9$ TeV are compared with p-$\overline{\text{p}}$ data from the UA5 experiment [7] and with p-p NSD data from the CMS experiment [8]. The result is consistent both with UA5 and CMS data.

The right panel of fig. 2 shows the measurement for $\sqrt{s} = 2.36$ TeV, compared to CMS NSD data [8] and to PYTHIA tune D6T (109) [9] and PHOJET [10] calculations. The ALICE results for NSD collisions are consistent with CMS measurements, systematically above the PHOJET curve and significantly higher than the PYTHIA tune D6T prediction. The pseudorapidity density measurements in the central region ($|\eta| < 0.5$), for both the event classes and at the two energies, are summarized in table I together with UA5 and CMS results and both model predictions.

TABLE I. – *Charged-particle pseudorapidity densities measured by ALICE in p-p collisions at* $\sqrt{s} = 0.9$ *and* 2.36 TeV *for INEL and NSD event classes, compared with CMS and UA5 data as well as with PYTHIA tune D6T and PHOJET predictions. For ALICE the first error is statistical and the second is systematic.*

	ALICE p-p	CMS p-p	UA5 p-$\overline{\text{p}}$	PYTHIA	PHOJET
$\sqrt{s} = 0.9\,\text{TeV}$					
INEL	$3.02 \pm 0.01^{+0.08}_{-0.05}$		3.09 ± 0.05	2.35	3.21
NSD	$3.58 \pm 0.01^{+0.12}_{-0.12}$	$3.48 \pm 0.02 \pm 0.13$	3.43 ± 0.05	2.85	3.67
$\sqrt{s} = 2.36\,\text{TeV}$					
INEL	$3.77 \pm 0.01^{+0.25}_{-0.12}$			2.81	3.76
NSD	$4.43 \pm 0.01^{+0.17}_{-0.12}$	$4.47 \pm 0.04 \pm 0.16$		3.38	4.20

The main contribution to the systematic uncertainties at 0.9 and 2.36 TeV comes from the limited knowledge of cross-section and kinematics of diffractive processes. At 7 TeV, due to the lack of experimental information about these processes, a different event class has been defined by requiring at least one charged particle in the pseudorapidity interval $|\eta| < 1$ (INEL $> 0_{|\eta|<1}$), minimizing the model dependence of the corrections.

Results at $\sqrt{s} = 7\,\text{TeV}$ are based on 300000 p-p collisions. Data at lower energies have been re-analyzed in order to normalize the results to the same event class. In fig. 3 the centre-of-mass energy dependence of the charged-particle pseudorapidity density for the INEL $> 0_{|\eta|<1}$ class is compared to the evolution for the INEL and NSD classes at lower energies [11].

The observed trend is similar to that observed between 0.9 and 2.36 TeV for inelastic and non-single-diffractive events, then with a stronger increase with the energy in the data with respect to the model predictions. In table II the pseudorapidity density values
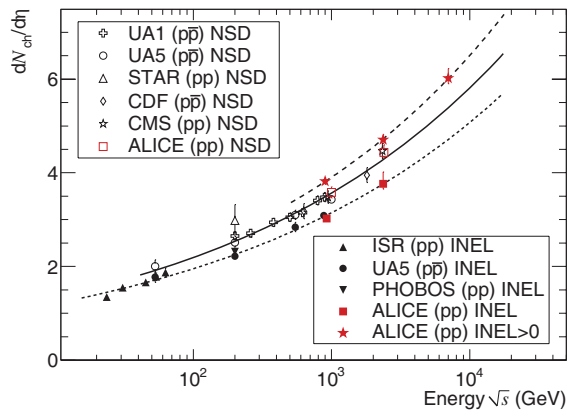

Fig. 3. – Charged-particle pseudorapidity density in $|\eta| < 0.5$ for INEL and NSD event classes and in $|\eta| < 1$ for the INEL $> 0_{|\eta|<1}$ event class, as a function of the centre-of-mass energy. The lines indicate the fit using a power-law dependence on energy [11].

TABLE II. – *Charged-particle pseudorapidity densities in p-p collisions at $\sqrt{s} = 0.9$, 2.36 and 7 TeV measured by ALICE for* INEL $> 0_{|\eta|<1}$ *event class, compared with different PYTHIA tunes and PHOJET predictions.*

Energy (TeV)	ALICE	PYTHIA			PHOJET
		(109)	(306)	(320)	
0.9	$3.81 \pm 0.01^{+0.07}_{-0.07}$	3.05	3.92	3.18	3.73
2.36	$4.70 \pm 0.01^{+0.11}_{-0.08}$	3.58	4.61	3.72	4.31
7	$6.01 \pm 0.01^{+0.20}_{-0.12}$	4.37	5.78	4.55	4.98

for $|\eta| < 1$ measured by ALICE at the three energies are reported and compared with predictions from different PYTHIA tunes (namely D6T (109), ATLAS-CSC (306) [12] and Perugia-0 (320) [13]) and from PHOJET.

An increase of 57.6% is observed going from the 0.9 to the 7 TeV data, compared with an increase of 47.6% obtained from the closest model (PYTHIA ATLAS-CSC) [11]. To better understand the increase from 0.9 to 2.36 TeV then to 7 TeV the multiplicity distributions for the INEL $> 0_{|\eta|<1}$ event class have been studied as well. In the left panel of fig. 4 the unfolded distributions at 0.9 and 2.36 TeV are well described by the Negative Binomial Distribution (NBD), while at 7 TeV the NBD fit slightly underestimates and overestimates the data at low and at high multiplicity, respectively.

The multiplicity distribution for the 7 TeV data is compared with models in the right panel of fig. 4: only PYTHIA tune ATLAS-CSC is close to the data at high multiplicity ($N_{ch} > 25$), even if it fails to reproduce the data in the intermediate region ($8 < N_{ch} < 25$). At low multiplicities, a large spread between the different models is observed, PHOJET being the lowest and PYTHIA tune Perugia-0 the highest [11].
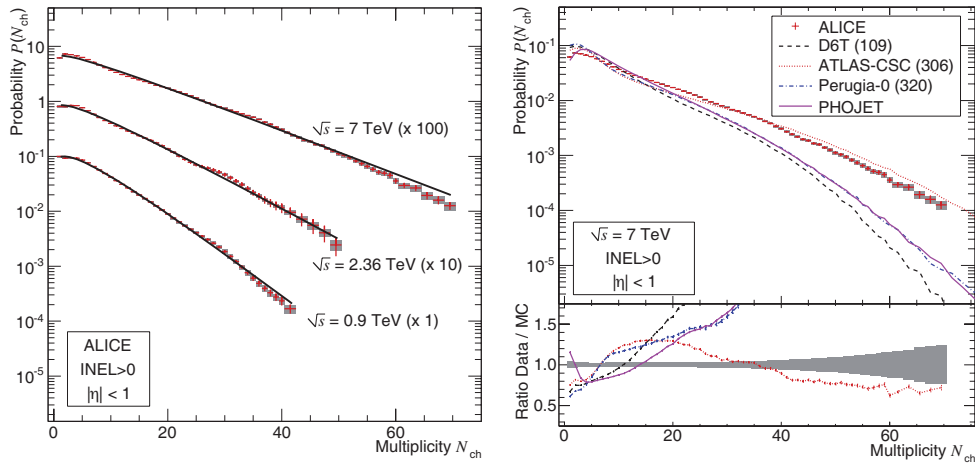

Fig. 4. – Left panel: multiplicity distributions in $|\eta| < 1$ for the INEL $> 0_{|\eta|<1}$ class at the three energies with the NBD fits. The error bars represent the statistical errors while the shaded areas represent the systematics. Right panel: data at $\sqrt{s} = 7$ TeV compared with models [11].

4. – Conclusions

The charged-particle pseudorapidity density and multiplicity distributions as measured by ALICE in p-p collisions at 0.9, 2.36 and 7 TeV centre-of-mass energy have been presented. The measured values of the pseudorapidity density at all energies are significantly larger than predicted by the current models, except for PYTHIA tune ATLAS-CSC. All the event generators significantly underpredict the pseudorapidity density increase with the energy. They also fail in reproducing the shape of the measured multiplicity distributions: the disagreement is not concentrated in a single region of the distribution and varies with the model.

REFERENCES

[1]   Alessandro B. *et al.* (ALICE Collaboration), *J. Phys. G*, **32** (2006) 1295.
[2]   Carminati F. *et al.* (ALICE Collaboration), *J. Phys. G*, **30** (2004) 1517.
[3]   Aamodt K. *et al.* (ALICE Collaboration), *J. Instrum.*, **3** (2008) S08002.
[4]   Aamodt K. *et al.* (ALICE Collaboration), *J. Instrum.*, **5** (2010) P03003.
[5]   Aamodt K. *et al.* (ALICE Collaboration), *Eur. Phys. J. C*, **65** (2010) 111.
[6]   Aamodt K. *et al.* (ALICE Collaboration), *Eur. Phys. J. C*, **68** (2010) 89.
[7]   Alner G. J. *et al.* (UA5 Collaboration), *Z Phys. C*, **33** (1986) 1.
[8]   Khachatryan V. *et al.* (CMS Collaboration), *JHEP*, **2010** (2010) 02041.
[9]   Albrow M. G. *et al.*, arXiv:hep-ph/0610012 (2006).
[10] Engel R. *et al.*, *Phys. Rev. D*, **52** (1995) 1459.
[11] Aamodt K. *et al.* (ALICE Collaboration), *Eur. Phys. J. C*, **68** (2010) 345.
[12] Moraes A., ATLAS Note ATL-COM-PYS-2009-119 (2009).
[13] Skands P. Z., arXiv:hep-ph/0905.3481 (2009).